Article

Using Geographic Information to Analyze Wildland Firefighter Situational Awareness: Impacts of Spatial Resolution on Visibility Assessment

Katherine A. Mistick [1],* , Philip E. Dennison [1] , Michael J. Campbell [1] and Matthew P. Thompson [2]

1   Department of Geography, University of Utah, Salt Lake City, UT 84112, USA
2   USDA Forest Service, Rocky Mountain Research Station, Fort Collins, CO 80526, USA
*   Correspondence: katherine.mistick@utah.edu

Abstract: Wildland firefighters must be able to maintain situational awareness to ensure their safety. Crew members, including lookouts and crew building handlines, rely on visibility to assess risk and communicate changing conditions. Geographic information systems and remote sensing offer potential solutions for characterizing visibility using models incorporating terrain and vegetation height. Visibility can be assessed using viewshed algorithms, and while previous research has demonstrated the utility of these algorithms across multiple fields, their use in wildland firefighter safety has yet to be explored. The goals of this study were to develop an approach for assessing visibility at the handline level, quantify the effects of spatial resolution on a lidar-driven visibility analysis, and demonstrate a set of spatial metrics that can be used to inform handline safety. Comparisons were made between elevation models derived from airborne lidar at varying spatial resolutions and those derived from LANDFIRE, a US-wide 30 m product. Coarser resolution inputs overestimated visibility by as much as 223%, while the finest-scale resolution input was not practical due to extreme processing times. Canopy cover and slope had strong linear relationships with visibility, with R^2 values of 0.806 and 0.718, respectively. Visibility analyses, when conducted at an appropriate spatial resolution, can provide useful information to inform situational awareness in a wildland fire context. Evaluating situational awareness at the handline level prior to engaging a fire may help firefighters evaluate potential safety risks and more effectively plan handlines.

Keywords: firefighter safety; handlines; situational awareness; visibility; lidar; LANDFIRE

1. Introduction

Wildland firefighter injuries and fatalities are unfortunately a routine occurrence [1,2]. One of the top five causes of firefighter fatalities is entrapment, when one or more firefighters become trapped by fire. While vehicle or stress-related incidents may be more common, entrapments have the potential to injure or kill large numbers of firefighters in a single incident, as was the case of the Yarnell Hill fire where 19 firefighters tragically lost their lives [3]. This tragedy unfolded in part due to the loss of situational awareness among the Granite Mountain Hotshots, who were traveling along an escape route towards a safety zone and lost sight of the fire. When the fire behavior shifted dramatically, the crew was caught unaware and became entrapped. Despite a long-term decrease in firefighter deaths from entrapment [2], multiple-fatality entrapment incidents remain a risk, particularly as firefighters are faced with managing increasingly large and complex fires [4–6].

One key protocol developed to improve firefighter safety is Lookouts, Communications, Escape Routes, and Safety Zones (LCES) [7]. Lookouts are experienced wildland firefighters assigned to specifically monitor changes—such as weather, fire behavior, and crew movement—that are indicative of potential hazards. Communication(s) stresses the importance of direct and prompt contact between firefighters and incident management. Escape routes are predefined paths to safety, of which there must be multiple options [8].

Lastly, safety zones are predefined areas of refuge should fire behavior introduce unsafe conditions [8]. Other guiding principles for improving safety in the US firefighting community include the 10 Standard Firefighting Orders and 18 Watch Out Situations, colloquially known as the 10s and 18s, which prompt fire personnel to improve decision making towards safer and more effective management [9].

A common thread throughout LCES and the 10s and 18s is the importance of maintaining situational awareness. Situational awareness, or one's dynamic perception of their surroundings, has been studied in detail for high-risk, constantly changing situations such as those found in the military [10,11], medical field [12,13], and firefighting [14,15]. Not only does situational awareness encompass the ability to perceive one's current situation, it also incorporates the ability to predict and respond to changes in a manner that best supports one's desired outcome [16]. In the case of wildland firefighting, this means constantly monitoring and reevaluating the environment, hazard, and safety protocols to minimize risk. However, maintaining situational awareness can be difficult due to the often unpredictable nature of fire behavior, firefighter qualifications and experience, topography, and human factors like organization and psychology [15,17].

Recent research has focused on improving firefighter safety by increasing our understanding of one or more aspects of situational awareness, as it pertains to wildland firefighting. Jolly & Freeborn [14] developed a framework for determining fire behavior risk rating to improve situational awareness, while other studies have focused on uncovering the effects of topography and fuel on entrapment potential [15,18,19]. Another area of research has focused on geospatial modeling of escape routes and safety zones, aiming to improve our understanding of travel rates [20–23] and spatial attributes of safety zones [24–26]. While many of these studies have covered critical aspects of LCES, one aspect that has gone largely unexamined is the importance of lookouts and their responsibility to maintain a line of sight to both crew and fire hazards, providing situational awareness by proxy to the crew. The importance of maintaining situational awareness, however, extends beyond just the lookouts, as any member of a fire crew has the ability and authority to alert others of perceived threats [7]. To ensure the safety of firefighters, it is important to direct lookouts and crew towards locations on the landscape from which visibility can be maintained.

While visibility is critical across many aspects of wildland fire management, it is especially important for wildland firefighters constructing handlines, which are a containment tactic that involves crew using handtools to remove vegetation and dig or scrape away any flammable materials along a continuous line so as to reduce unwanted fire spread (Figure 1, [8]). Handlines vary widely in both length and width, depending heavily on fire behavior, fuel type, and containment needs; they are typically linear features that tend to avoid midslopes and may align with features such as roads, trails, or ridges [27]. Identifying suitable handlines is a multifaceted problem that requires considering the suppression difficulty, the potential for successful containment, the ease of egress, and the accessibility of a suitable safety zone [20,24,28,29]. Geospatial analysis can contribute to mapping and quantifying these considerations. However, of comparable importance to these considerations is the ability of the crew to maintain situational awareness based on local landscape conditions. To date, there have been no known attempts to use geographic information systems and remote sensing to assess visibility at the handline level.

Figure 1. Example of handline construction in a forested landscape. © Bureau of Land Management Oregon and Washington, "SCOFMP Guard School 2013", 18 June 2013, accessed from Flickr. Licensed with CC BY-SA 2.0.

In a wildland environment, local and landscape-level terrain and vegetation structure influence not only visibility but also management decisions that direct the crew's activity on the landscape. For example, the National Wildfire Coordinating Group (NWCG) Instructor Guide on Handline Technique specifically mentions hazardous terrain that should be avoided when constructing handlines, "locate line away from features such as drop offs, steep slopes, chimneys, and chutes" [27]. Therefore, a quantitative understanding of local topography is critical for maintaining situational awareness when fighting wildland fires. Further, the third Standard Firefighting Order says that one must, "base all actions on current and expected behavior of the fire." [9], and it is well understood that changes in slope can directly influence fire behavior [30]. Multiple of the 18 Watch Out Situations emphasize the need to understand surrounding fuels in order to maintain situational awareness [9,30]. Metrics relating to surrounding fuels include canopy cover and canopy height. In combination, understanding both terrain and vegetation structure can inform and improve situational awareness in addition to providing information on potential obstructions to visibility. Our analysis uses geographic information systems and remote sensing to address both visibility from handlines and the terrain and vegetation characteristics surrounding handlines. The objectives of this study are to:

- Introduce an approach for quantifying visibility at the scale of wildland firefighter handlines.
- Determine the effect of spatial resolution of lidar-derived elevation data on calculated visibility in a forested environment and evaluate implications for wildland firefighter safety assessment.
- Use geospatial information to assess the general safety and situational awareness of handlines based on landscape metrics and visibility.

2. Background

One of the best sources of data for mapping terrain and vegetation structure is lidar, an active remote sensing technique that uses pulsed laser light to measure elevation of the ground and aboveground features [31]. Millions of points, each with an x, y, and z coordinate, form a three-dimensional point cloud with the density of data dictating the amount of spatial detail captured [31]. Point clouds can be rasterized to produce elevation models inclusive of vegetation (digital surface models (DSMs)) or exclusive of vegetation (digital terrain models (DTMs)). DTMs are useful for mapping not only elevation, but also many derivative topographic features, including the slope and topographic position across a landscape. Topographic position index (TPI) indicates relative elevation, relying on the elevation of a central pixel and the average elevation of a surrounding annulus with predefined inner and outer radii [32,33]. A positive TPI indicates the location is relatively elevated above its surrounding landscape, such as a ridge or hilltop. Conversely, a negative value indicates relatively low elevation, such as a valley or canyon bottom. Larger radii will

provide a broader regional context for relative elevation quantification, whereas smaller radii will provide a more local account of topographic position. TPI, especially when used in conjunction with slope, can illuminate areas that are potentially hazardous (e.g., varying TPIs indicating rugged terrain, low negative TPIs indicating a valley bottom).

In vegetated environments, lidar pulses can often produce multiple point returns, with the first return representing the elevation of the highest aboveground reflective surface that the pulse interacted with (e.g., the top of a tree canopy) and the last return representing the lowest surface. Using a ground point classification algorithm, each point in a cloud can be classified as being either "ground" or "non-ground" [34,35]. While DTMs are interpolated from only ground-classified points, DSMs are interpolated from first-return points to allow for the incorporation of above-ground features, such as vegetation height, in addition to the terrain elevation. Subtracting DTM elevations from DSM elevations at the pixel-level produces a canopy height model (CHM). CHMs contain spatially exhaustive, per-pixel representations of vegetation height across entire landscapes—a critical fuel structural measure. Canopy cover is determined by dividing the total number of pixels above a certain canopy height threshold by the total number of pixels within an area of given dimensions. Not only can DSMs provide quantitative fuels information, but they can provide further detail on potential obstructions to visibility. By incorporating all ground and aboveground elevations, DSMs can be used to assess visibility across a landscape by serving as the elevation model over which a viewshed is calculated [36,37].

In this study, we use viewsheds to assess visibility, an important component of situational awareness, along handlines. A viewshed is calculated as the sum of all possible lines of sight from a given perspective, accounting for any obstructions between the observer and a pre-defined maximum distance of interest. If no intermediate obstructions are present in the line of sight to a target (an object or landscape feature), the target would be considered visible. If any intermediate obstruction (i.e., an elevation above the line of sight) is present, the target will not be visible (Figure 2). Viewsheds have been used across many disciplines including archeology, landscape and urban planning, social sciences, and environmental science [36–41]. While previous research has shown the usefulness of viewshed algorithms in applications across fields, their use in wildland firefighter safety has yet to be explored. However, viewshed analysis may help wildland firefighters identify areas from which large proportions of the landscape can be seen, giving firefighters the opportunity to maintain a line-of-sight with members of their crew, other proximal crews, ground resources, and the fire. Conversely, viewshed analysis may also help identify high-risk areas from which relatively small proportions of the landscape can be seen.

As with many geospatial analyses, one of the most important considerations in conducting a viewshed analysis is the spatial resolution of the input data. Coarse resolutions tend to oversimplify the landscape, while providing the benefit of faster data processing, whereas fine resolutions tend to capture much more spatial detail, at the expense of processing efficiency. Thus, it is important to consider what resolution is suitable for viewshed analyses in the context of wildland firefighter safety. One study has specifically looked at how spatial resolution interacts with viewsheds: Vukomanovic et al. [37] found that coarse resolutions tend to overestimate visibility, when calculating viewsheds from the perspective of housing developments in exurban (low-density, with population growth) spaces. While relevant, their work focused on single observer viewsheds in increasingly populated areas. Our research aims to apply similar methods using multiple observers, across multiple handlines to further understand the best resolution for visibility calculations but also the feasibility and application of these analyses for improving wildland firefighter situational awareness and safety.
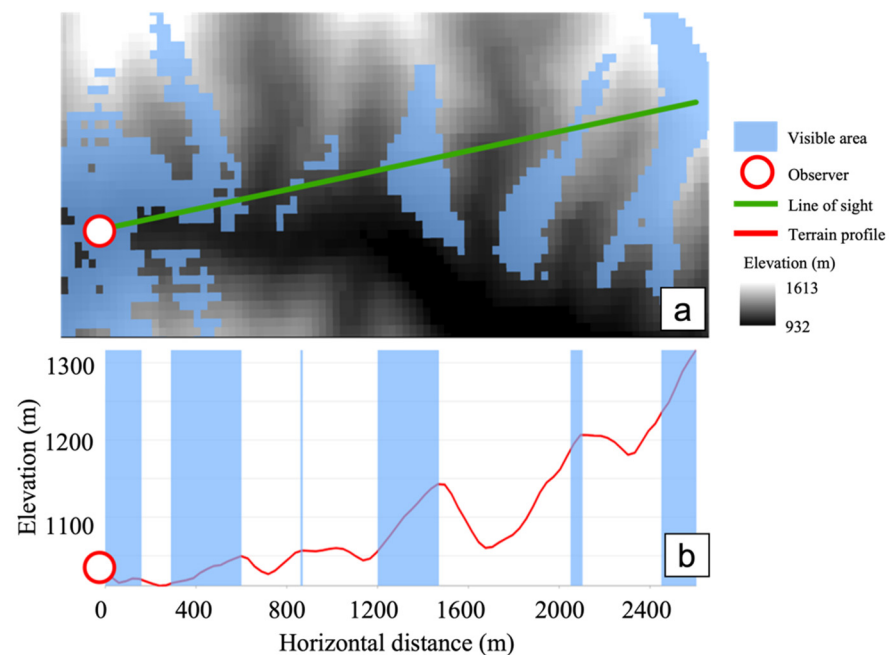
Figure 2. Viewshed schematic. (**a**) Map of elevation overlaid with viewshed results indicating visible pixels (blue) calculated from the observer. Green line indicates a single line of sight. (**b**) Aligned terrain profile of line of sight (red line) with blue shading indicating visible features.

3. Materials and Methods

3.1. Study Area

The Green Ridge fire in southeastern Washington, USA (Figure 3) was ignited by lightning on 7 July 2021, and served as the case study for this analysis. Growing to over 174 km^2, this fire had nearly 400 assigned personnel during peak fire activity and was not contained until 21 October 2021 [42]. Elevation in the immediate vicinity of the fire ranges from approximately 924 m to 1942 m. Official fire updates described the topography of the area as steep and rugged, with rolling rocks and burning material requiring the modification of tactics to prioritize firefighter and public safety [42].
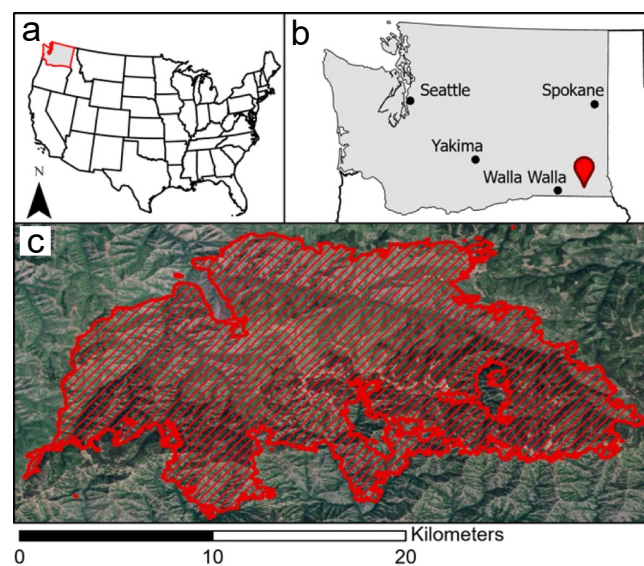
Figure 3. Green Ridge fire location. (**a**) Washington, USA. (**b**) Red pin indicates the fire location in southeastern Washington. (**c**) Cross-hatched area indicates one of the last infrared-captured fire perimeters for the Green Ridge fire, on 12 September 2021.

The pre-fire landscape was tree-dominated, with LANDFIRE Existing Vegetation Type classifying most of the area as a mixed conifer forest including Douglas fir (Pseudotsuga menziesii), ponderosa pine (Pinus ponderosa), and lodgepole pine (Pinus contorta). Some shrub-dominated areas exist, predominantly classified as sagebrush steppe, within the immediate vicinity of the fire as well. Overall heavy fuels combined with active fire behavior in rugged terrain required complex management of the Green Ridge fire, making it a useful study area for this analysis and generally representative of wildfires in rough, forested terrain in the western United States.

3.2. Data

3.2.1. Digital Elevation Models

Four spatial resolutions of digital elevation model (DEM) were considered in this study: 1, 5, 10, and 30 m. These DEMs were derived from USGS 3DEP airborne lidar data [43], acquired prior to the fire between fall of 2017 and summer of 2018. All lidar products used in this study meet at least the QL2 quality level requirements [44], meaning they have a nominal pulse density of at least two points per square meter, and a vertical accuracy of 10 cm. The average point density of this dataset is 8.06 pts/m^2, and the entire final Green Ridge fire perimeter and surrounding landscape is captured by this product. Point clouds were accessed from USGS and processed using LAStools [45]. A 1 m resolution DSM (including vegetation height) and a 1 m DTM (excluding vegetation height) were generated directly from the point cloud, with coarser resolutions (5, 10, 30) generated by aggregating the rasterized model according to pixel means. Note that DEM, DSM, DTM, and other acronyms used in this paper are defined in Abbreviations part.

A second 30 m resolution elevation model was derived by adding LANDFIRE Existing Vegetation Height (EVH) to a USGS-produced DTM from Shuttle Radar Topography Mission (SRTM) data [46] to produce a DSM. EVH is a modeled vegetation height representing the average height of the dominant vegetation within each 30 m pixel. While our resolution comparison will focus on varying lidar-derived resolutions, lidar products have limited spatial and temporal availability, whereas EVH and SRTM data provide nationwide coverage with EVH updates approximately every two years. By including a EVH and SRTM-derived DSM in our analysis, we can provide realistic commentary on how using these more widely available data sources could affect results.

3.2.2. Handlines

Handline locations were acquired from the geospatial incident data provided by the National Interagency Fire Center for the Green Ridge fire. Five completed handlines were selected for analysis (Figure 4, Table 1). Handlines are referred to using the date they were added to geospatial incident data. While it may be useful to know the visibility from every possible point along a handline, there are a potentially infinite number of locations from which visibility could be assessed along a continuous line. Further, crew locations change throughout a shift as a handline is completed, and the precise position of crew along a line at any given time may unpredictable. Thus, we defined a set of observer point locations (hereby referred to as nodes), placed every 90 m along the handline features (Figure 4). We note that the minimum practical node spacing that could be used in our analysis is 30 m, corresponding with the coarsest spatial resolution examined. However, 30 m node spacing imposes significant processing requirements. We selected 90 m node spacing to balance accurately representing crew locations on each handline with processing efficiency.
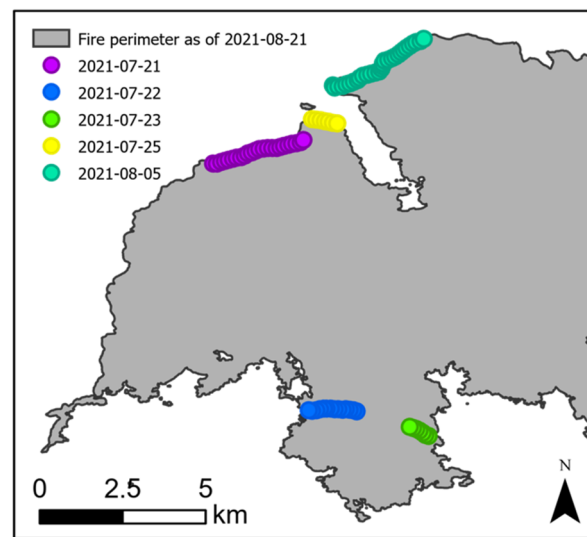
Figure 4. Locations of handline crew nodes (circles), color-coded by date. A Green Ridge fire perimeter from 2021-08-21 is shown for reference.

Table 1. Summary of nodes used for Green Ridge fire handlines.

Handline	Number of Crew Nodes	Fire Growth [1] (Hectares)	Total Fire Area [1] (Hectares)
2021-07-21	24	679	1313
2021-07-22	14	270	1583
2021-07-23	7	271	1853
2021-07-25	7	270	2381
2021-08-05	30	501	5458

[1] Values acquired from Green Ridge incident reports [42].

3.3. Viewshed Processing

All viewshed processing was done using the ArcPy (Esri, Redlands, CA, USA) library in Python 3.7.9. Geodesic Viewshed (also referred to as "Viewshed 2") was used to calculate all viewsheds in ArcGIS Pro 2.7 (Esri, Redlands, CA, USA) [47]. This algorithm accounts for the curvature of Earth's surface by transforming surface elevations into three-dimensional coordinates and calculating geodesic sightlines [47]. Geodesic Viewshed requires an input elevation model and observer point location (s). For this analysis, DSMs of varying resolution were used as input elevation models, accounting for the effects of both terrain and vegetation on visual obstruction. Observer height, an optional input, was defined as 1.7 m per node to account for average human height. Viewshed radius, another optional input, was restricted to 3.5 km per node to capture a sufficiently large area useful for fire management objectives while tempering computational demands.

For each handline, viewsheds were calculated at four resolutions (1, 5, 10 and 30 m) in order to evaluate the effects of spatial resolution on the assessment of visibility. Additional 30 m viewsheds were calculated for each handline using the LANDFIRE/SRTM-derived DSM. Particularly at high spatial resolutions and over large areas, viewshed calculations require an immense number of calculations. To increase performance, Geodesic Viewshed calculations were implemented using a Nvidia Tesla T4 graphics processing unit with 320 tensor cores and 16 GB of memory.

Geodesic Viewshed outputs a raster indicating visible pixels on the landscape, according to input nodes and elevation model. Viewsheds and their derivatives can be summarized by a series of equations:

$$V = \begin{cases} 1 \ \text{if visible} \\ 0 \ \text{if invisible} \end{cases} \tag{1}$$

$$V_c = \frac{\sum_{i=1}^{n} V_i}{n} \qquad (2)$$

$$V_{c,x} = \begin{cases} 1 \ if \ V_c \geq x \\ 0 \ if \ V_c < x \end{cases} \qquad (3)$$

$$VI_x = \frac{\sum_{j=1}^{m} V_{c,x}}{m} \qquad (4)$$

where V represents binary visibility of viewshed raster pixels (Equation (1)), V_c is a composite viewshed representing the proportion of crew nodes $V_i = \{i, \dots, n\}$ that can "see" each pixel on the landscape, and $V_{c,x}$ is a binary classification of V_c with a proportional threshold x applied (e.g., 50%). Two thresholded composite viewsheds were calculated using Equation (3): $x = 25\%$ ($V_{c,0.25}$) and $x = 50\%$. ($V_{c,0.5}$). V_c (Equation (2)) is the composite viewshed based on at least one node being able to see pixels on the landscape, whereas $V_{c,0.25}$ and $V_{c,0.5}$ require that at least quarter or half of nodes be able to see pixels on the landscape, providing a higher level of situational awareness along a handline. VI_x (Equation (4)) is the visibility index [48] representing the proportion of pixels that can be seen from a handline based on all pixels in the viewshed radius $\{j, \dots, m\}$. Visibility index is equivalent to percent of pixels visible on the landscape from handline nodes and was analyzed for each handline and resolution combination. VI was calculated both using no threshold (referred to simply as VI) and using 0.25 and 0.5 threshold values for x ($VI_{0.25}$, $VI_{0.5}$). Resolution comparisons were done by plotting lidar-derived VIs as a function of resolution across all five handlines. Lidar-derived VIs at 30 m were also compared with LANDFIRE/SRTM-derived VIs at 30 m by fitting linear regressions, grouped by threshold level, across all five handlines.

3.4. Handline Landscape Metrics

Four landscape metrics (Table 2) were calculated in order to assess general characteristics and safety of each handline: slope, canopy height (CH), canopy cover, and topographic position index (TPI). Metrics were only considered at 5 m spatial resolution in order to be consistent with the ultimate resolution selected from the visibility analysis. Slope was derived from a 5 m DTM generated from lidar data (3.2.1). CH was also lidar-derived, by subtracting 5 m DTM values from 5 m DSM values to generate a 5 m raster of heights. Only values over 1.37 m, a typical breast height used in dendrometric measurements, were considered part of the canopy. Percent canopy cover relies on CH values to determine the proportion of vegetated pixels above that same height threshold. TPI was calculated from the 5 m DTM using an outer radius of 12 pixels (60 m) and an inner radius of 6 pixels (30 m), providing a local assessment of relative elevation.

Table 2. Summary of landscape metrics.

Landscape Metric	Definition	Derived from
Slope	The gradient or steepness of a surface	DTM
Canopy height (CH)	Height of vegetation across a landscape	CHM
Canopy cover	Proportion of the landscape covered by vegetation of a certain height	CHM
Topographic position index (TPI)	Relative elevation, relies on the elevation of a central pixel and the average elevation of a surrounding annulus with predefined inner and outer radii [32,33]	DTM

Each metric was determined for raster cells within a 50 m buffer zone surrounding each handline feature (Figure 5). This buffer was selected to account for both the potential spatial uncertainty in the handline spatial feature and to gain a sense of the terrain and vegetation conditions not only along the line but in the immediate vicinity of the line. All but canopy cover (a percentage) were reported as distributions of values with the median used for comparisons, owing to its robustness against outliers. Handline metrics were compared with VI to determine potential influences of these metrics on visibility. Linear

regressions were applied to VI as a function of canopy cover, median canopy height, median slope, and median TPI, all within the 50 m handline buffer.
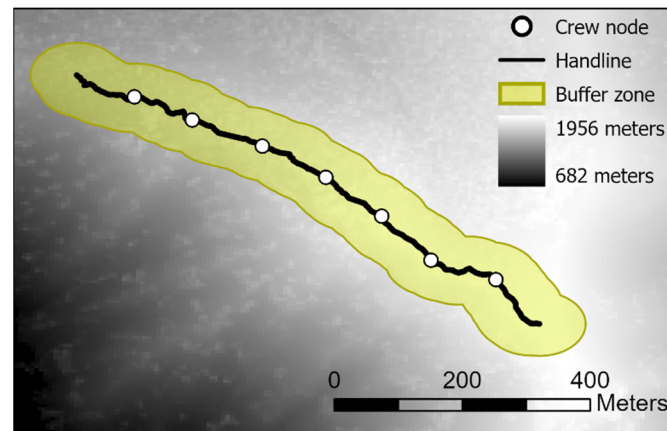
Figure 5. Buffer zone showing the area over which handline landscape metrics are calculated. Handline 2021-07-23 used as example. The background is the 5 m DSM.

4. Results

Overall, our viewshed analysis determined there was limited visibility from handlines within the study area, with rugged, forested terrain dictating the spatial distribution of areas with higher or lower visibility (Figure 6a). Figure 6a shows the spatial arrangement of V_c where $n = 14$ (Equation (2)) and where the predominant direction of visibility is towards the west, with the highest V_c values concentrated in the southwest. The introduction of thresholds further spatially restricts viewsheds but also highlights areas visible to a higher percentage of crew nodes (Figure 6b,c). Processing times for 1 m viewsheds could exceed 10 h depending on the number of nodes used. Not only were these processing times potentially unrealistic, but a single 1 m viewshed also required up to 3.6 GB of storage space. On the other hand, 5 m viewshed processing times were on the scale of minutes, and storing these viewsheds required just 0.29 GB of space.
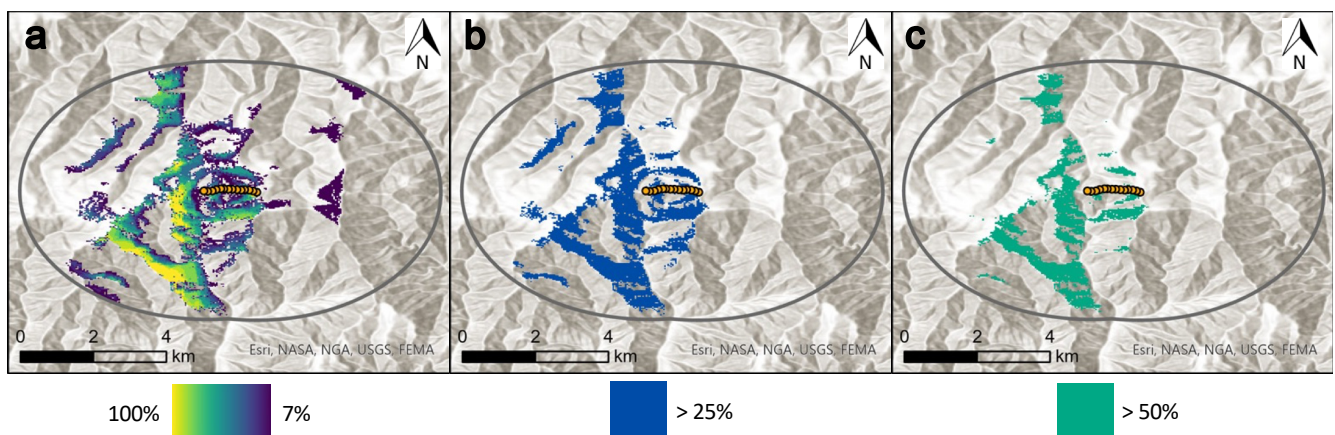

Figure 6. Example viewshed outputs, calculated using a 30 m LANDFIRE-derived DSM, for the 2021-07-22 handline. Gray boundary represents viewshed radius. (**a**) V_c, indicating areas visible to any node, with shading indicating the percent of nodes visible to each pixel. (**b**) $V_{c,0.25}$, indicating areas visible to at least 25% of nodes. (**c**) $V_{c,0.5}$, indicating areas visible to at least 50% of nodes.

4.1. Effect of Spatial Resolution of Elevation Data on Calculated Visibility

Across all five handlines, VI was highest when using 30 m DSMs, followed by 10 and 5, with 1 m consistently reporting the lowest VI (Figure 7a). Relative to 1 m, VI was overestimated by an average of 75% at 5 m, 133% at 10 m, and 223% at 30 m. The 2021-08-05

handline, with 30 crew nodes, reported the highest VI, with as much as 38.28% of the landscape visible at 30 m resolution. This same handline resulted in the highest 1 m VI with 14.95% of the landscape visible. The 2021-07-23 handline, with seven crew nodes, consistently reported the lowest VI with just 12.71% of the landscape visible at 30 m and 0.15% of the landscape visible at 1 m. Notably, the 2021-07-25 handline, also just 718 m in length, reported the third-highest VI, across all resolutions (Figure 7a). This suggests that length is not the singular driver of VI and that other landscape factors are likely introducing complexity and obscuring visibility across various lengths of handlines.
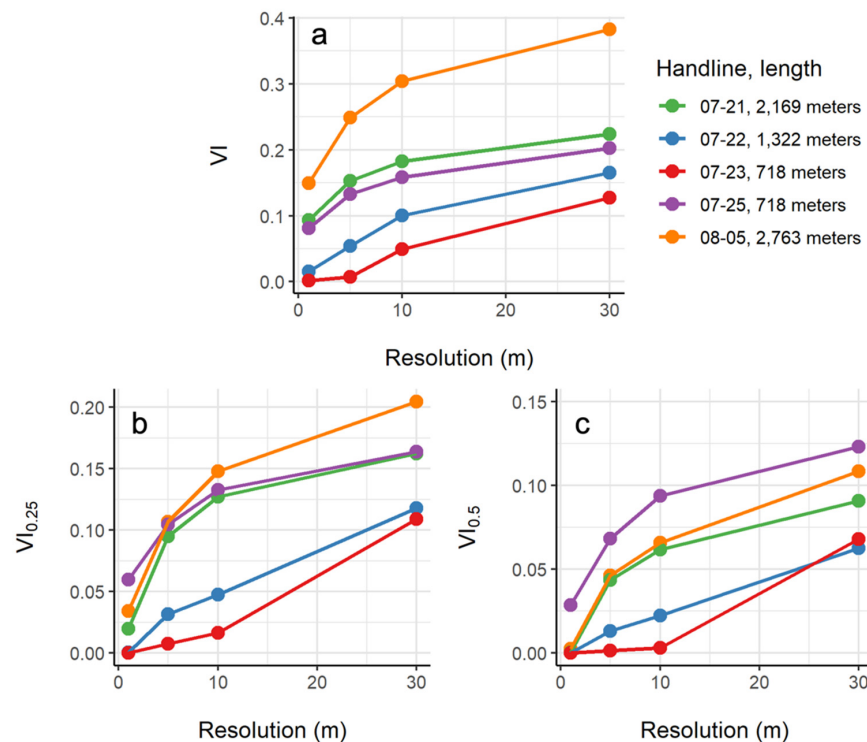

Figure 7. VI across resolutions. Connected points represent VI derived from lidar-based viewsheds for each handline. (**a**) VI, no threshold. (**b**) $VI_{0.25}$, $x = 25\%$ threshold applied. (**c**) $VI_{0.5}$, $x = 50\%$ threshold applied.

When introducing a 25% threshold, visibility decreased across all handlines and resolutions, with 2021-08-05 retaining the highest $VI_{0.25}$, 20.5%, at 30 m (Figure 7b). However, 2021-08-05 did not retain the highest $VI_{0.25}$ across all resolutions. At 1 m 2021-07-25 reported the highest $VI_{0.25}$, 6%, surpassing both 2021-08-05 (3.4%) and 2021-07-21 (2%). 2021-07-25 also surpassed 2021-07-21 at 5 m resolution, reporting 10.4% compared with 9.5%, respectively. This indicates that at 1 m the 2021-07-21 handline has a larger proportion of highly visible areas (VI > 0.25) than the other four handlines.

The introduction of a 50% threshold further decreased $VI_{0.5}$ with a new maximum of 12.3% of the landscape visible for 2021-07-25 at 30 m resolution (Figure 7c). At this threshold, across all handlines and resolutions, 2021-07-25 consistently reported the highest $VI_{0.5}$ despite having the fewest crew nodes.

While coarsening resolution led to increased VIs across all lidar-derived models, the VIs for the LANDFIRE/SRTM DSM were generally less than those of the lidar-based 30 m models (Figure 8). Exclusive of 2021-07-22, all handlines, regardless of threshold, produced a lower percent of the landscape visible using 30 m LANDFIRE/SRTM, suggesting a consistent underestimation of VI by LANDFIRE/SRTM. 2021-07-22, a moderately long handline at 1322 m, was the only handline to produce greater VI using lidar than LANDFIRE/SRTM, at both no threshold and 50% threshold. While all linear relationships had slopes <1, the relationship between 30 m lidar-derived VI and LANDFIRE/SRTM-derived VI with no threshold applied resulted in the strongest correlation ($R^2 = 0.87$, $p = 0.02$) (Table 3).
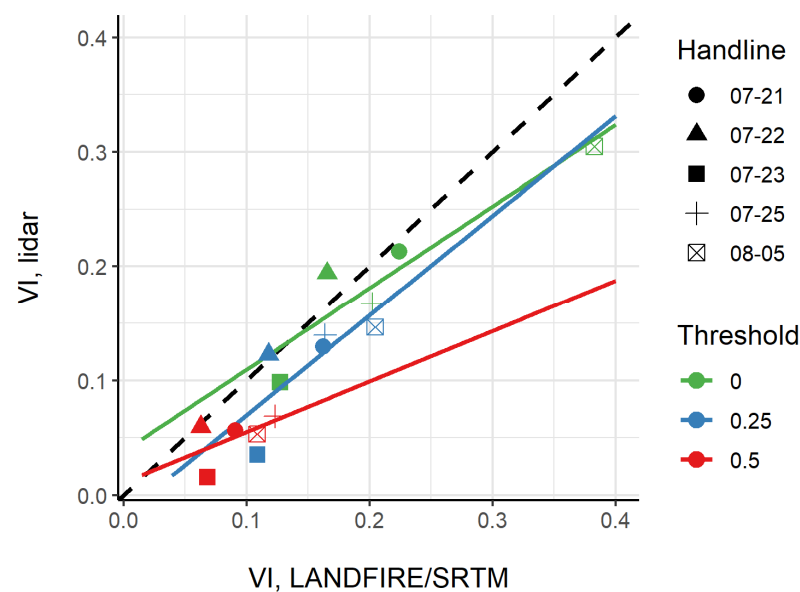
Figure 8. Comparison of 30 m lidar-derived VIs and LANDFIRE/SRTM-derived *VIs*. VI for each handline (marker shape) is plotted 3 times, once per threshold (marker color). Dashed line indicates a slope of 1. Dashed black line indicates a slope of 1.

Table 3. Summary statistics for linear regressions in Figure 8.

Threshold	Slope	y-Intercept	R^2	*p*-Value
0	0.72	3.79	0.87	0.02
0.25	0.87	−1.74	0.56	0.15
0.5	0.44	1.08	0.31	0.33

4.2. Handline Landscape Metrics

As visibility analysis demonstrated that 5 m resolution data had greatly reduced processing times when compared with more precise 1 m data, landscape metrics were calculated at 5 m resolution. Table 4 provides the summary statistics for landscape metrics calculated for each handline. Across all five handline buffer zones, canopy cover ranged from 25.33% to as much as 64.59% (Table 4). VI had a strong negative correlation with percent canopy cover ($R^2 = 0.806$) but was not strongly correlated with median canopy height ($R^2 = 0.202$) or median TPI ($R^2 = 0.06$). Higher canopy cover introduces more instances of vegetation obstructing lines of sight in a viewshed, whereas once vegetation heights are tall enough to block a line of sight, their continued height over that threshold is irrelevant, resulting in the relatively poor correlation for canopy height. A fairly strong positive correlation between VI and median slope was observed ($R^2 = 0.718$), with 2021-07-25 acting as an outlier, having the highest median slope but only the third-highest VI (Table 4). The presence of steep slopes reduces visibility as steep slopes readily obstruct lines of sight.

Table 4. Summary of handline metrics.

Handline	Length (m)	Canopy Cover (%)	Median Canopy Height (m)	Median Slope (Degrees)	Median TPI	VI [1]
2021-07-21	2169	26.27	3.69	30.07	14.62	0.153
2021-07-22	1322	60.89	8.14	21.54	9.83	0.054
2021-07-23	718	64.59	5.56	19.16	13.91	0.007
2021-07-25	718	28.83	3.57	32.43	10.01	0.133
2021-08-05	2763	25.33	5.16	30.79	13.71	0.249

[1] VI is derived from non-thresholded viewsheds processed using 5 m, lidar-derived DSMs.

Distributions of canopy height, slope, and TPI are plotted in Figure 9, arranged in rows by handline, including values for canopy cover and visibility. These distributions

provide much more information than median values and illustrate key differences between handlines, which allowed us to determine which factors were potentially influencing visibility and which factors may contribute to the overall safety of the area in which a handline is built. For example, the range of median TPI was just 4.79, but the range of values across all handlines was [−35.5, 80.9] (Figure 9). Despite relatively similar median TPI values (relatively small, positive), the distributions of TPI help differentiate each handline and indicate potential safety concerns. The 2021-07-25 handline (Figure 9d) had a trimodal TPI distribution with one peak occurring at approximately −10, another near +10, and a third near +30, suggesting the immediate landscape surrounding this landscape contains a concentration of both ridge and valley features. Handlines from 2021-07-21 and 2021-07-22 (Figure 9a,b) had distinctly unimodal TPI distributions with medians of 14.62 and 9.83, respectively, suggesting they are relatively positioned above their immediate surroundings.
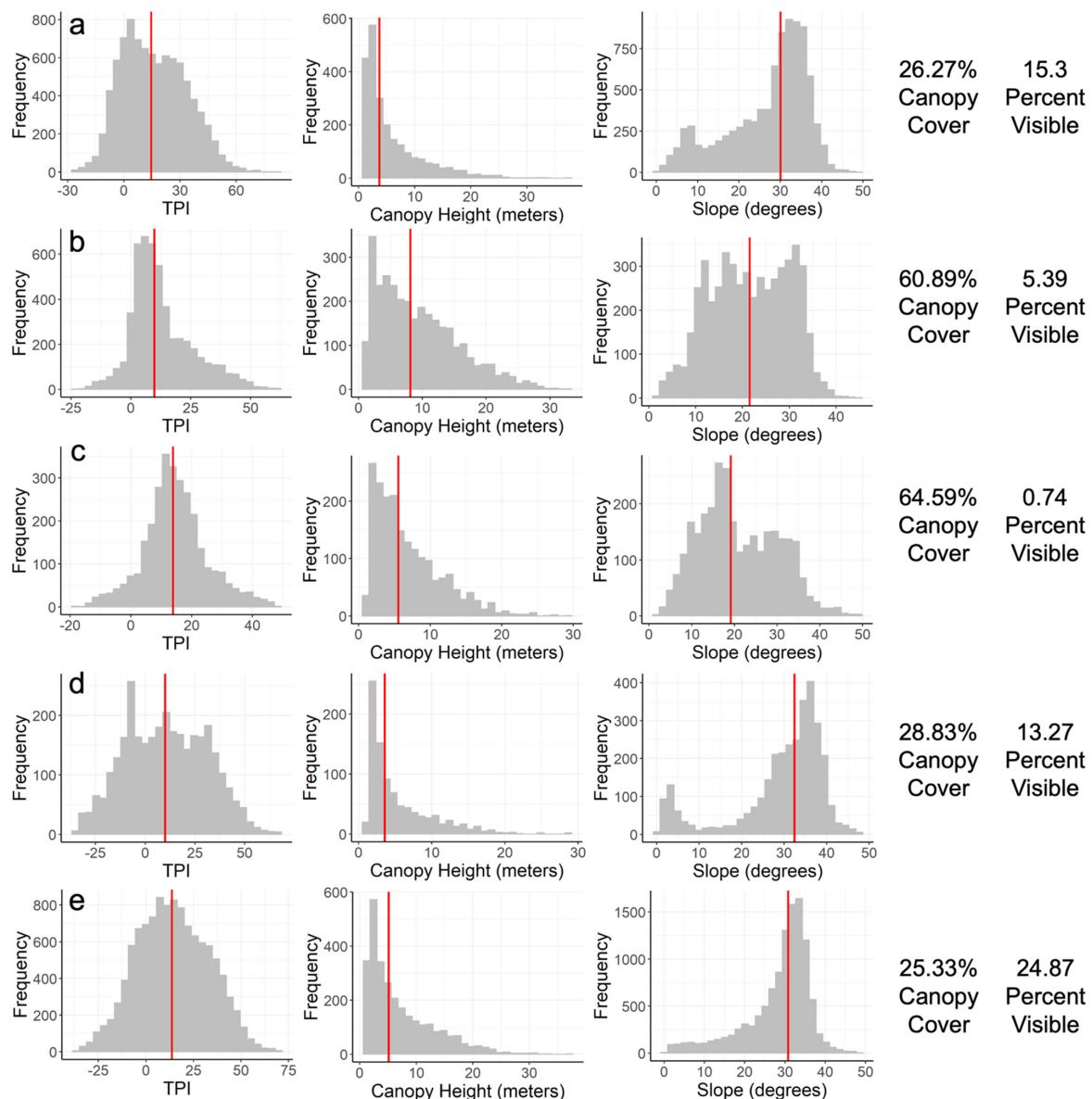
Figure 9. Distributions of handline metrics where frequency (*y*-axis) refers to the number of occurrences of each variable (*x*-axis) in the designated buffer zone. Percent visible was derived from non-thresholded viewsheds processed using 5 m, lidar-derived DSMs, where percent visible = $VI \times 100$. (Row (**a**)) 2021-07-21. (Row (**b**)) 2021-07-22. (Row (**c**)) 2021-07-23. (Row (**d**)) 2021-07-25. (Row (**e**)) 2021-08-05.

Handlines with higher percentages of the landscape visible (2021-07-21, 2021-07-25, 2021-08-05) had the three lowest median canopy heights, but again the range of these values across all five handlines was quite small. Noticeably, these three handlines had canopy height distributions of distinctly similar shapes: a strong, narrow, left skew with a very narrow tail out to about 20 m (Figure 9a,d,e). Handlines 2021-07-22 and 2021-07-23, on the other hand, had strong, but much wider, left skews suggesting presence of taller vegetation throughout these areas (Figure 9b,c). Both were nearly bi-modal, having small secondary peaks >10 m.

The three handlines with higher VI also shared similar distributions of slope: a strong right skew with a median near 30 degrees. While the handline with the highest VI was unimodal, both 2021-07-21 and 2021-07-25 were bi-modal with secondary peaks between 0 and 10 degrees (Figure 9a,d,e). 2021-07-22 and 2021-07-23, the lowest VI handlines, had consistently wider distributions, with the distribution of slope values for 2021-07-22 being tri-modal, and 2021-07-23 having a moderate left skew and slight bi-modal distribution (Figure 9b,c).

5. Discussion

Our analysis demonstrated that coarsening spatial resolution led to an increase in VI, which represents the percent of the landscape that is visible to one or more observers along a handline. These coarser resolution elevation models tended to oversimplify landscapes in terms of both terrain and vegetation obstructions. Due to the overestimation of visibility at coarser resolutions, it is tempting to select the finest spatial resolution as the ideal resolution for visibility analyses. However, despite the fact that the 1 m data produced the most limited visibility (therefore also the least-overestimated), our results suggest that 5 m may be a better resolution for applied use due to significantly decreased processing times, while retaining considerable spatial detail.

Regardless of spatial resolution, these analyses are limited by their reliance on precisely located but arbitrarily placed node locations. While handline selection was purposeful and node placement was designed to capture spatial variation along the handline, the specific node locations restrict visibility by not accounting for between-node visibility and the spatial uncertainty of the drawn handline. Realistically, a firefighter could traverse an area in the vicinity of the handline to find the best vantage point, and these small changes in observer location will influence the resulting viewshed and visibility [49]. While changes in observer location influence visibility, the length of a handline (and therefore the number of observers) does not necessarily improve visibility. Especially when implementing thresholds, we saw that one of the shortest handlines retained the greatest amount of visibility (Figure 7c). This suggests that other variables such as canopy cover and slope, rather than handline length or number of nodes, may be more important when considering visibility. Further, this study was conducted on a fire in the Pacific Northwest region of the United States, a densely forested and rugged landscape. Viewshed analyses applied to fires in other ecosystems—with lower relief terrain and different fuel types, for example—may result in fewer differences across resolutions, with slope and canopy cover having more or less influence. Future work could consider modeling continuous visibility across a variety of landscapes, allowing for an understanding of the influence of local changes in node location and environmental influences on visibility.

While fine-scale spatial resolution may be ideal for visibility analysis, data with sub-10 m spatial resolution have limited spatial and temporal availability. LANDFIRE 30 m products, on the other hand, are available across the United States and are more frequently updated to reflect current conditions. This justifies our comparison between lidar-derived DSMs and LANDFIRE-derived DSMs, of which we found the latter to generally underestimate visibility. This underestimation may be due to inherent differences in the data sources: lidar is directly measured whereas LANDFIRE EVH is modeled based on a combination of multispectral imagery, lidar, and ancillary datasets [50]. Further, there are three recent historical fires within 3.5 km of one or more of the handlines considered in this study that

affect the vegetation structure: the Butte Creek Fire, ignited 14 August 2015, the Columbia Complex, ignited 21 August 2006, and the School Fire, ignited 5 August 2005 [51]. It is possible that LANDFIRE overestimated post-fire recovery of these areas, reporting taller vegetation heights, thus leading to an underestimation of visible area. Future work could further investigate post-fire discrepancies between LANDFIRE EVH and lidar-derived canopy height. While 30 m resolution lidar-derived DSMs significantly overestimated visibility, LANDFIRE/SRTM-derived visibility was less severe in its overestimation and may be an acceptable alternative when finer-scale spatial resolution is unavailable. Ultimately lidar coverage is preferred for these types of analyses due to the ability to select spatial resolution at an appropriate level and to capture canopy height most accurately. However, even where lidar coverage is available, the timing of lidar acquisition remains a concern due to vegetation disturbance and regrowth resulting in changing vegetation height and canopy cover over time.

Slopes surrounding the handlines examined in this case study were relatively steep, and could present challenges in traversing the landscape [20,21] in addition to producing potentially dangerous fire behavior. Planning for slopes and topographic conditions is critical for wildland firefighters, as was the case of the 2020 Silverado fire entrapment, where multiple crew suffered critical burn injuries and major damage to their PPE when they were mid-slope and were overrun by fire running upslope [52]. This burnover incident highlighted lessons learned including, "Evaluate topography when establishing control lines" and "Recognize the alignment of the (fuel, wind, and topography) factors that influence wildland fire behavior" [52]. In the 2013 Yarnell Hill fire, where multiple fatalities resulted from entrapment in a box canyon, steep slopes made travel difficult, obscuring visibility, and reducing situational awareness [3]. The 2021 McFarland fire entrapment, where crew members became entrapped while suppressing spot fires along a planned containment line, specifically highlight lookouts and situational awareness in the lessons learned published in the facilitated learning analysis, writing that, "Those involved emphasized the importance of lookouts that have a vantage point capable of seeing where danger may come from" [53].

While topography and visibility contributed to these incidents, it's important to acknowledge that other factors also likely played a role, including (but not limited to) smoke, wind, weather, fuel moisture, and fire behavior [3,52,53]. We note that geographic information cannot address all aspects of situational awareness, including varying qualifications and experience levels of firefighters affecting decision-making, or the oftentimes erratic nature of fire behavior [15,17]. However, smoke impacts on visibility may be readily addressable using viewshed analysis. This study assumed a static viewshed radius of 3.5 km from each node. While crew members may be able to see 3.5 km or more on a clear sky day, the radius used in this study could significantly overestimate visibility in smoky conditions. The viewshed radius could be varied to account for reduced visibility due to smoke. Future work should investigate how to take smoke impacts on visibility into account for viewshed calculation, and potentially introduce a dynamic viewshed radius to account for smoke effects.

While not all handline metrics saw strong correlations with visibility, both canopy cover and median slope saw strong negative and positive correlations, respectively, which indicates that further visibility analyses might consider these variables. While we did not observe a strong relationship between visibility and median canopy height or median TPI, these variables are still important for planning and understanding existing safety protocols. The distributions of each variable could be considered in a real-time dashboard format, along with canopy cover, slope, and a map of visibility, to inform crews and incident command of local conditions (Figure 10). Current management strategies could be enhanced by incorporating this dashboard concept that would provide a quantitative summary of the potential hazards crews may face (Figure 10).
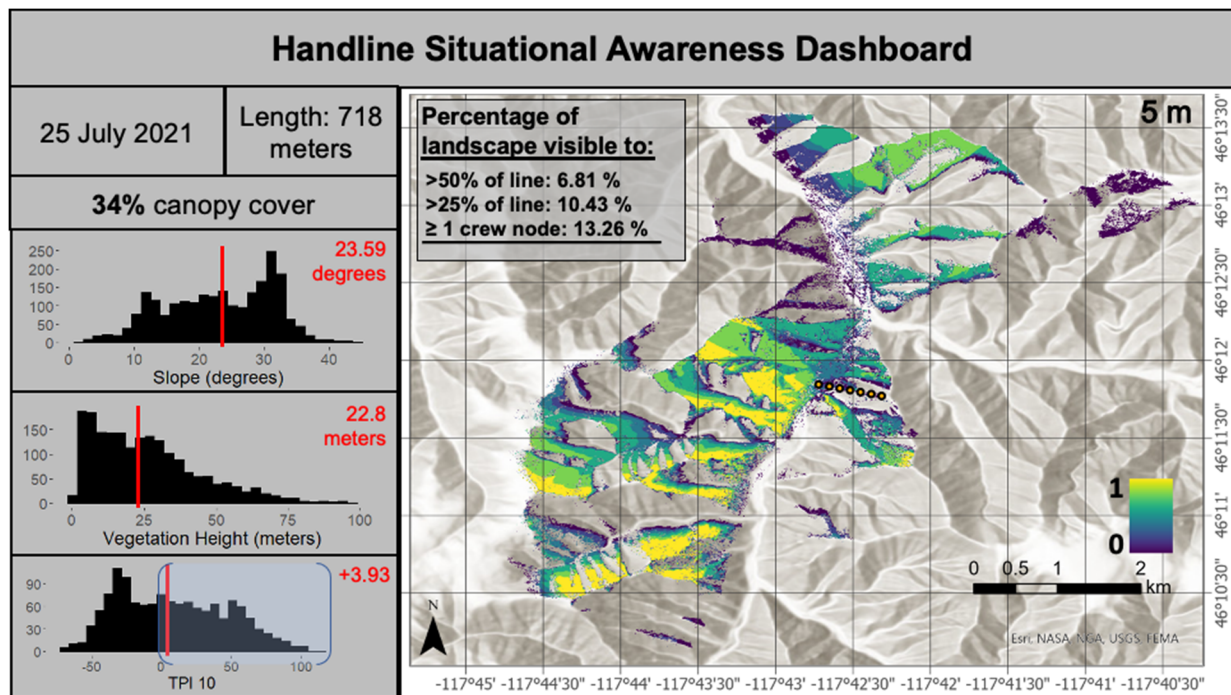
Figure 10. Mockup of a dashboard incorporating visibility, canopy cover, slope, vegetation height, and TPI. Blue brackets in overlaid on the TPI histogram highlight areas of higher elevation relative to the immediate surroundings.

6. Conclusions

Maintaining situational awareness is paramount to wildland firefighters' safety while working on a fire. Many protocols and training initiatives, such as LCES and the 10 s and 18 s, provide a framework for evaluating hazards such as dangerous terrain or fuel. However, identifying and assessing these variables relies on a wildland firefighter or incident manager's training, experience, and familiarity with local landscape characteristics. This study demonstrates how geographic information systems and remotely sensed data can be used to analyze one component of situational awareness, visibility, and provide a series of relevant landscape metrics surrounding handlines prior to engaging a fire. Quantitative and spatially explicit evaluations of these important safety metrics could enable fire crews to make comparisons between different potential handline options, choosing those which will ensure the crew can maximize their situational awareness when suppressing a fire.

Overall, we found that:

- Estimating visibility at the handline level through viewshed analysis can assist wildland firefighters with evaluating potential limitations to situational awareness
- Spatial resolution has a pronounced effect on the estimation of visibility and therefore must be taken into consideration prior to use in fire management operations
- Coarser resolution DSMs ($\geq$10 m), including those created from lidar data and from more widely available LANDFIRE and SRTM products, likely overestimate visibility
- Viewshed analysis conducted at a spatial resolution of 5 m provides a high degree of landscape structural detail while significantly reducing processing time and storage requirements as compared to the same analysis conducted at finer resolutions (1 m)
- Canopy cover and slope displayed strong linear relationships with visibility
- Landscape metrics, when presented in conjunction with visibility analyses, offer the potential to improve situational awareness and/or inform management decisions

Our results demonstrated that spatial resolution is an important consideration when performing a visibility analysis to determine the relative proportions of the landscape that can and cannot be seen from a given vantage point. While the finest spatial resolution

data available will provide the most realistic, yet consistently most conservative results, this spatial resolution is not always feasible nor available. Where available, lidar provides accurate elevation data at varying spatial resolutions, depending on each point cloud's inherent attributes such as pulse density, allowing users to specify an appropriate resolution for their analyses. In this study, 5 m spatial resolution was selected as the resolution that reached a balance between accuracy and computational intensity. However, airborne lidar data are not universally available; therefore 30 m LANDFIRE EVH was compared with 30 m lidar. While both significantly overestimated visibility, EVH estimated lower visibility than that of 30 m lidar, likely due to different methods used for determining height, and potentially influenced by nearby historical burns.

When visibility is analyzed in conjunction with other landscape metrics such as slope, TPI, canopy height, and canopy cover, handline safety may be assessed using quantitative distributions to inform fire management decisions. We found that increasing canopy cover led to decreased visibility, and decreased slope led to increased visibility. While other variables did not reveal strong relationships with visibility, their distributions still collectively informed the general safety of an area by revealing trends in TPI and canopy height across handlines. This proposed combination of landscape metrics could be applied in a dashboard format to quickly provide this information in real time to land or incident managers.

Future applications of viewshed analysis for firefighter safety could examine visibility along wider containment lines cleared by heavy equipment, taking into account visibility along the cleared width of the line, along escape routes, and within safety zones. Viewshed analysis may also assist with determining optimal locations of lookouts to maintain visibility of both crew and wildfire.

Author Contributions: Conceptualization K.A.M., P.E.D. and M.J.C.; methodology K.A.M., P.E.D. and M.J.C.; software, K.A.M.; formal analysis, K.A.M.; resources, P.E.D., M.J.C. and K.A.M.; data curation, K.A.M.; writing—original draft preparation, K.A.M.; writing—review and editing, K.A.M., P.E.D., M.J.C. and M.P.T.; visualization, K.A.M.; supervision, P.E.D.; project administration, K.A.M., P.E.D.; funding acquisition, M.J.C., P.E.D. and M.P.T. All authors have read and agreed to the published version of the manuscript.

Institutional Review Board Statement: Not applicable.

Informed Consent Statement: Not applicable.

Conflicts of Interest: The authors declare no conflict of interest.

Abbreviations

Acronym	Significance
CH	Canopy height
CHM	Canopy height model
DEM	Digital elevation model
DSM	Digital surface model
DTM	Digital terrain model
EVH	Existing Vegetation Height
LCES	Lookouts, Communications, Escape Routes, Safety Zones
NWCG	National Wildfire Coordinating Group
SRTM	Shuttle Radar Topography Mission
TPI	Topographic Position Index
VI	Visibility Index

References

1. Page, W.G.; Freeborn, P.H.; Butler, B.W.; Jolly, W.M. A Review of US Wildland Firefighter Entrapments: Trends, Important Environmental Factors and Research Needs. *Int. J. Wildland Fire* **2019**, *28*, 551. [CrossRef]
2. National Wildfire Coordinating Group. NWCG Report on Wildland Firefighter Fatalities in the United States: 2007–2016. 2017. Available online: https://www.nwcg.gov/sites/default/files/publications/pms841.pdf (accessed on 6 September 2022).
3. Arizona State Forestry Division. Yarnell Hill Serious Accident Investigation Report. 2013. Available online: https://wildfiretoday. com/documents/Yarnell_Hill_Fire_report.pdf (accessed on 15 September 2022).
4. Abatzoglou, J.T.; Battisti, D.S.; Williams, A.P.; Hansen, W.D.; Harvey, B.J.; Kolden, C.A. Projected Increases in Western US Forest Fire despite Growing Fuel Constraints. *Commun. Earth Environ.* **2021**, *2*, 227. [CrossRef]
5. Balch, J.K.; Schoennagel, T.; Williams, A.P.; Abatzoglou, J.T.; Cattau, M.E.; Mietkiewicz, N.P.; Denis, L.A.S. Switching on the Big Burn of 2017. *Fire* **2018**, *1*, 17. [CrossRef]
6. Dennison, P.E.; Brewer, S.C.; Arnold, J.D.; Moritz, M.A. Large Wildfire Trends in the Western United States, 1984–2011. *Geophys. Res. Lett.* **2014**, *41*, 2928–2933. [CrossRef]
7. Gleason, P. Lookouts, Communication, Escape Routes and Safety Zones, "LCES". 1991. Available online: https://www.nwcg. gov/sites/default/files/wfldp/docs/lces-gleason.pdf (accessed on 28 September 2022).
8. NWCG Glossary of Wildland Fire. Available online: https://www.nwcg.gov/glossary/a-z (accessed on 6 September 2022).
9. California Conversvation Corps. 10 Standard Orders & 18 Watch Outs. 2019. Available online: https://ccc.ca.gov/wp-content/ uploads/2019/08/CCC-10-Standard-Orders-18-Watch-Outs.pdf (accessed on 6 September 2022).
10. Baek, H.; Lim, J. Design of Future UAV-Relay Tactical Data Link for Reliable UAV Control and Situational Awareness. *IEEE Commun. Mag.* **2018**, *56*, 144–150. [CrossRef]
11. Nofi, A. *Defining and Measuring Shared Situational Awareness*; Center for Naval Analyses: Alexandria, VA, USA, 2000.
12. Gillespie, B.M.; Gwinner, K.; Fairweather, N.; Chaboyer, W. Building Shared Situational Awareness in Surgery through Distributed Dialog. *J. Multidiscip Healthc* **2013**, *6*, 109–118. [CrossRef] [PubMed]
13. Graafland, M.; Schraagen, J.M.C.; Boermeester, M.A.; Bemelman, W.A.; Schijven, M.P. Training Situational Awareness to Reduce Surgical Errors in the Operating Room. *Br. J. Surg.* **2014**, *102*, 16–23. [CrossRef] [PubMed]
14. Jolly, W.M.; Freeborn, P.H. Towards Improving Wildland Firefighter Situational Awareness through Daily Fire Behaviour Risk Assessments in the US Northern Rockies and Northern Great Basin. *Int. J. Wildland Fire* **2017**, *26*, 574. [CrossRef]
15. Page, W.G.; Butler, B.W. Fuel and Topographic Influences on Wildland Firefighter Burnover Fatalities in Southern California. *Int. J. Wildland Fire* **2018**, *27*, 141. [CrossRef]
16. Stanton, N.A.; Chambers, P.R.G.; Piggott, J. Situational Awareness and Safety. *Saf. Sci.* **2001**, *39*, 189–204. [CrossRef]
17. Mangan, R. *Investigating Wildland Fire Entrapments*; United States Department of Agriculture: Missoula, MT, USA, 1995.
18. Lahaye, S.; Sharples, J.; Matthews, S.; Heemstra, S.; Price, O.; Badlan, R. How Do Weather and Terrain Contribute to Firefighter Entrapments in Australia? *Int. J. Wildland Fire* **2018**, *27*, 85. [CrossRef]
19. Page, W.G.; Freeborn, P.H.; Butler, B.W.; Jolly, W.M. A Classification of US Wildland Firefighter Entrapments Based on Coincident Fuels, Weather, and Topography. *Fire* **2019**, *2*, 52. [CrossRef]
20. Campbell, M.J.; Page, W.G.; Dennison, P.E.; Butler, B.W. Escape Route Index: A Spatially-Explicit Measure of Wildland Firefighter Egress Capacity. *Fire* **2019**, *2*, 40. [CrossRef]
21. Campbell, M.J.; Dennison, P.E.; Butler, B.W.; Page, W.G. Using Crowdsourced Fitness Tracker Data to Model the Relationship between Slope and Travel Rates. *Appl. Geogr.* **2019**, *106*, 93–107. [CrossRef]
22. Campbell, M.J.; Dennison, P.E.; Butler, B.W. A LiDAR-Based Analysis of the Effects of Slope, Vegetation Density, and Ground Surface Roughness on Travel Rates for Wildland Firefighter Escape Route Mapping. *Int. J. Wildland Fire* **2017**, *26*, 884. [CrossRef]
23. Sullivan, P.R.; Campbell, M.J.; Dennison, P.E.; Brewer, S.C.; Butler, B.W. Modeling Wildland Firefighter Travel Rates by Terrain Slope: Results from GPS-Tracking of Type 1 Crew Movement. *Fire* **2020**, *3*, 52. [CrossRef]
24. Campbell, M.J.; Dennison, P.E.; Thompson, M.P.; Butler, B.W. Assessing Potential Safety Zone Suitability Using a New Online Mapping Tool. *Fire* **2022**, *5*, 5. [CrossRef]
25. Campbell, M.J.; Dennison, P.E.; Butler, B.W. Safe Separation Distance Score: A New Metric for Evaluating Wildland Firefighter Safety Zones Using Lidar. *Int. J. Geogr. Inf. Sci.* **2017**, *31*, 1448–1466. [CrossRef]
26. Dennison, P.E.; Fryer, G.K.; Cova, T.J. Identification of Firefighter Safety Zones Using Lidar. *Environ. Model. Softw.* **2014**, *59*, 91–97. [CrossRef]
27. National Wildfire Coordinating Group. S-130 Unit 9: Handline Techniques. In *NWCG Instructor Guide*; pp. 1–22. Available online: https://training.nwcg.gov/dl/s130/s-130-ig09.pdf (accessed on 15 September 2022).
28. O'Connor, C.D.; Calkin, D.E.; Thompson, M.P. An Empirical Machine Learning Method for Predicting Potential Fire Control Locations for Pre-Fire Planning and Operational Fire Management. *Int. J. Wildland Fire* **2017**, *26*, 587. [CrossRef]
29. Rodríguez y Silva, F.; O'Connor, C.D.; Thompson, M.P.; Molina Martínez, J.R.; Calkin, D.E. Modelling Suppression Difficulty: Current and Future Applications. *Int. J. Wildland Fire* **2020**, *29*, 739. [CrossRef]
30. National Interagency Fire Center. Chapter 7: Safety and Risk Management. In *Interagency Standards for Fire and Fire Aviation Operations*; 2022. Available online: https://www.nifc.gov/sites/default/files/redbook-files/Chapter07.pdf (accessed on 15 September 2022).

31. Lefsky, M.A.; Cohen, W.B.; Parker, G.G.; Harding, D.J. Lidar Remote Sensing for Ecosystem Studies. *BioScience* **2002**, *52*, 19. [CrossRef]

32. Gallant, J.C.; Wilson, J.P. Primary Topographic Attributes. In *Terrain Analysis: Principles and Applications*; John Wiley & Sons Inc.: Hoboken, NJ, USA, 2000; Volume 7, pp. 51–85. ISBN 0-471-32188-5.

33. Weiss, A. Topographic Position and Landforms Analysis. In Proceedings of the ESRI Users Conference, San Diego, CA, USA, 12 July 2001.

34. Evans, J.S.; Hudak, A.T. A Multiscale Curvature Algorithm for Classifying Discrete Return LiDAR in Forested Environments. *IEEE Trans. Geosci. Remote Sens.* **2007**, *45*, 1029–1038. [CrossRef]

35. Meng, X.; Currit, N.; Zhao, K. Ground Filtering Algorithms for Airborne LiDAR Data: A Review of Critical Issues. *Remote Sens.* **2010**, *2*, 833–860. [CrossRef]

36. Murgoitio, J.J.; Shrestha, R.; Glenn, N.F.; Spaete, L.P. Improved Visibility Calculations with Tree Trunk Obstruction Modeling from Aerial LiDAR. *Int. J. Geogr. Inf. Sci.* **2013**, *27*, 1865–1883. [CrossRef]

37. Vukomanovic, J.; Singh, K.K.; Petrasova, A.; Vogler, J.B. Not Seeing the Forest for the Trees: Modeling Exurban Viewscapes with LiDAR. *Landsc. Urban Plan.* **2018**, *170*, 169–176. [CrossRef]

38. Bartie, P.; Reitsma, F.; Kingham, S.; Mills, S. Incorporating Vegetation into Visual Exposure Modelling in Urban Environments. *Int. J. Geogr. Inf. Sci.* **2011**, *25*, 851–868. [CrossRef]

39. Yu, S.; Yu, B.; Song, W.; Wu, B.; Zhou, J.; Huang, Y.; Wu, J.; Zhao, F.; Mao, W. View-Based Greenery: A Three-Dimensional Assessment of City Buildings' Green Visibility Using Floor Green View Index. *Landsc. Urban Plan.* **2016**, *152*, 13–26. [CrossRef]

40. Chamberlain, B.C.; Meitner, M.J. A Route-Based Visibility Analysis for Landscape Management. *Landsc. Urban Plan.* **2013**, *111*, 13–24. [CrossRef]

41. Fisher, P.; Farrelly, C.; Maddocks, A.; Ruggles, C. Spatial Analysis of Visible Areas from the Bronze Age Cairns of Mull. *J. Archaeol. Sci.* **1997**, *24*, 581–592. [CrossRef]

42. Green Ridge Fire. Available online: https://inciweb.nwcg.gov/incident/7628/ (accessed on 6 September 2022).

43. Sugarbaker, L.; Constance, E.W.; Heidemann, H.K.; Jason, A.L.; Saghy, D.L.; Stoker, J.M. *The 3D Elevation Program Initiative—A Call for Action*; USGS: Reston, VA, USA, 2014.

44. Topographic Data Quality Levels (QLs). Available online: www.usgs.gov/3d-elevation-program/topographic-data-quality-levels-qls (accessed on 6 September 2022).

45. Isenburg, M. *LAStools*; Rapidlasso GmbH: Gilching, Germany, 2015.

46. Farr, T.G.; Kobrick, M. Shuttle Radar Topography Mission Produces a Wealth of Data. *Eos Trans. Am. Geophys. Union* **2000**, *81*, 583–585. [CrossRef]

47. ESRI. How Geodesic Viewshed Works. Available online: https://pro.arcgis.com/en/pro-app/2.8/tool-reference/spatial-analyst/how-viewshed-2-works.htm (accessed on 6 September 2022).

48. Franklin, W.R.; Ray, C.K. Higher Isn't Necessarily Better: Visibility Algorithms and Experiments. *Adv. GIS Res.* **1994**, *2*, 22.

49. Campbell, M.J.; Dennison, P.E.; Hudak, A.T.; Parham, L.M.; Butler, B.W. Quantifying Understory Vegetation Density Using Small-Footprint Airborne Lidar. *Remote Sens. Environ.* **2018**, *215*, 330–342. [CrossRef]

50. Existing Vegetation Height, LF 2016 Remap [LF 2.0.0]. Available online: https://landfire.gov/evh.php (accessed on 6 September 2022).

51. Data Access: Fire Level Geospatial Data. Available online: https://mtbs.gov/direct-download (accessed on 6 September 2022).

52. Orange County California Fire Authority Informational Summary Report of Serious or Near Serious Injuries, Illnesses and Accidents—Firefighter Burn Over October 26, 2020 Silverado Incident. 2020. Available online: https://wildfiretoday.com/documents/Green-Sheet-OCFA-Final-_1_.pdf (accessed on 15 September 2022).

53. USDA Forest Service, Pacific Southwest Region, Shasta-Trinity National Forest. *Is That the Freight Train I'm Hearing?* McFarland Fire Entrapment FLA. 2021. Available online: https://www.wildfirelessons.net/HigherLogic/System/DownloadDocumentFile.ashx?DocumentFileKey=64ec35f7-9ee7-48f5-a821-be3d9f6a3738&forceDialog=0 (accessed on 15 September 2022).